Autophagy-related signature as Indicators for the Prognosis of Hepatocellular carcinoma

Wen Ye
Wenzhou Medical University
Zhehao Shi
Wenzhou Medical University
Zhongjing Zhang
Wenzhou Medical University
Yi Zhou
Wenzhou Medical University
Bicheng Chen
Wenzhou Medical University
Qiyu Zhang (Qiyuz@126.com)
https://orcid.org/0000-0001-5463-6459

Primary research

Keywords: HCC, Autophagy, TCGA, ICGC, Prognostic signature

Posted Date: June 4th, 2020

DOI: https://doi.org/10.21203/rs.3.rs-32431/v1

Abstract

Background

Hepatocellular carcinoma (HCC) is the most common and deadly type of liver cancer. Autophagy is the process of transporting damaged or aging cellular components into lysosomes for digestion and degradation. There is an accumulative evidence implies that autophagy is a key factor of the progression of cancer. The aim of this study was to determine a panel of a novel autophagy-related prognostic marker for liver cancer.

Methods

We conducted a comprehensive analysis of ARGs expression profiles and corresponding clinical information based on The Cancer Genome Atlas (TCGA) and International Cancer Genome Consortium (ICGC) database. The univariate Cox proportional regression model was used to screen candidate autophagy-related prognostic genes. In addition, the multivariate Cox proportional regression model were helped to prove five key prognostic autophagy-related genes (ATIC, BAX, BIRC5, CAPNS1 and FKBP1A), which were used to construct prognostic signature.

Results

Based on the prognostic signature, liver cancer patients were significantly divided into high-risk and low-risk groups in terms of overall survival (OS). Further multivariate Cox regression analysis indicated that the prognostic signature remained as an independent prognostic factor for OS. The prognostic signature in possession of a better Area Under Curves (AUC) has a better performance in predicting the survival of patients with HCC, compared with other clinical parameters.

Conclusion

This study provides a prospective biomarker for monitoring the outcomes in the patients with HCC.

Background:

Liver cancer is one of the most common malignant tumors in alimentary (digestive) system with poor clinical prognosis, and also the second leading cause of cancer-related mortality [1]. Hepatocellular carcinoma (HCC) accounts for 75%-85% of primary liver cancer cases, which make it the most common type of liver cancer [1]. Liver cancer patients were often diagnosed at a late stage so that the efficacy or result of operation was limited and dispirited. Thus, it is crucial to explore an effective therapeutic indicator to achieve better prognosis in clinic. The correlation between autophagy and HCC has been

studied, showing a new direction and approach for clinical treatment of liver cancer. For example, it was demonstrated that autophagy can induce resistance of HCC cells to chemotherapeutic agents [2, 3].

Autophagy is the process of transporting damaged, denatured or aging cellular components into lysosomes for digestion and degradation. Autophagy is an approach or process regulating cell metabolism and maintains homeostasis, and participating in a variety of pathophysiological processes including malignant tumors. However, the efficacy of autophagy in cancer still inconclusive, whereas it has been reported that autophagy acts a dual function in the development of tumors. On the one hand, autophagy degradation of cellular components can provide nutrient supply for tumor cell survival. On the other hand, it can inhibit tumorigenesis by clearing toxic cellular materials. To date, researchers on autophagy and liver cancer mainly focus on cancer progression and chemotherapy resistance [4–6]. However, the role of autophagy in liver cancer prognosis has rarely been explored.

In this study, we established a signature involving five autophagy-related genes (ARGs) to predict prognosis in the patients with liver cancer, and found that it was an independent prognostic index for liver patients. Through our study, it is suggested that ARGs play important roles in liver cancer and may show potential and valuable performance for predicting the prognosis of HCC patients.

Material And Methods

Data acquisition

A total of 232 ARGs was obtained from the Human Autophagy Database (HADb, http://autophagy.lu/clustering/index.html). The transcription factors (TFs) information, gene-expression profiles and the clinical data of liver cancer cohort were obtained from TCGA portal (https://portal.gdc.cancer.gov/) and ICGC portal (http://dcc.icgc.org/releases/current/Projects) respectively. At the same time, the samples acquired from the TCGA dataset were listed as the training group and those from the ICGC dataset as validation cohort.

Identification of differentially expressed ARGs

It was conducted that the differential ARGs expression analysis between HCC and normal liver tissue by using the “limma” package of R. Genes with false discovery rate (FDR) < 0.05 and |log2 fold change (FC)| > 1 was considered to be the significantly differentially expressed ARGs. Then Venn diagram was used to detect overlapping target genes.

Differentially expressed ARGs enrichment analysis

Kyoto Encyclopedia of Genes and Genomes (KEGG) pathway genome and gene ontology (GO) genome were selected to conduct a series of gene functional enrichment analysis to find the major biological attributes. In addition, we employed the GOplot package for visualing the enrichment terms.

Construction of OS risk prognostic model based on ARGs

Initially, the potential prognostic ARGs related to liver cancer patients' OS were selected by univariate Cox regression analyses. Next, using multivariate Cox regression analyses to explore whether these candidate prognostic genes can be independent predictors of prognosis monitoring in TCGA cohorts. Finally, several prognostic ARGs were selected (out or excluded) and Cox proportional hazards regression was employed to build the OS risk prognostic model. The autophagy-related risk score for each patient was calculated by relative expression value multiplied regression coefficients. X-tile analysis was used to select optimal cutoff value in the training group. Simultaneously, the HCC patients were separated into low-risk and high-risk groups according to the value. The overall survival was assessed by using Kaplan–Meier curve. Then, the differences in survival were estimated into high- or low-lrisk groups based on log-rank test.The Cox regression model was employed to analyze the factors affecting the OS in patients with HCC. The risk score, age, gender, cancer grade, cancer stages were used as covariates.

Statistical analysis

The cut-off point for risk score was determined by X-tile 3.6.1 software, based on the minimal P value. Statistical analysis was performed with R software. Receiver operating characteristic (ROC) curve was used to estimate prognostic value of the risk score. AUC value equal to or greater than 0.7 were regarded a significant predictive value. P value < 0.05 was considered as significant.

Results

Identification of differentially expressed ARGs

After extracting the expression values of 232 ARGs of liver cancer patients, 32 and 64 differentially expressed ARGs were identified in TCGA and ICGC database respectively (Fig. 1). Furthermore, the expression pattern of differentially expressed ARGs between the HCC tissues and normal tissues in these two databases were visualized by scatter plots (Fig. 2a, b). Venn diagram was used to find the ARGs that differentially expressed both in TCGA and ICGC database (Fig. 2c). Finally, we revealed 22 common differentially expressed ARGs in the two datasets, consisting of 3 upregulated genes (DIRAS3, FOS, ITGA3) and 19 down-regulated genes (ATIC, BAK1, BAX, BIRC5, CANX, CAPN1, CAPNS1, CCL2, FKBP1A, HSP90AB1, ITGA6, MAPK3, NAMPT, PARP1, PEA15, PRKCD, RPTOR, SPHK1, VAMP7).

Following differentially expressed TF genes were screened in TCGA and ICGC database respectively, Venn diagram was performed to find the intersection (Fig. 3a-c). Then a co-expression network was established with these differentially expressed TF genes and ARGs (Fig. 3d). The results showed that differentially expressed ARGs were co-expressed interactively with ERG1, ERG2 and FOXM1, etc.

Functional enrichment evaluation of the differentially expressed ARGs

The functional enrichment analysis of those differentially expressed ARGs was performed by GO and KEGG pathway, which elucidated the biological functions (Figs. 4 and 5). The top enriched GO annotation

were related to peptidyl-serine modification, regulation of protein binding and regulation of binding during the biological process. Cellular components included pseudopodium, pore complex, and integrin complex. And for molecular function, the terms of BH domain binding, SMAD binding, and chaperone binding were the top three. The KEGG enrichment pathways ware notably associated with Apoptosis, Colorectal cancer, Shigellosis, Platinum drug resistance, Protein processing in endoplasmic reticulum, and so on. Most of the Z-score of enriched pathways were less than zero, suggesting that most of them would be decreased. For ARGs differential express genes, the KEGG pathways including the IL-17 signaling pathway and the AGE – RAGE signaling pathway were displayed by heat-map.

Identification of prognostic ARGs

To reveal the relationship between the prognosis of patients and differential ARGs profiles, we evaluated the data obtained from TCGA by univariate Cox regression analysis. 14 ARGs were found significantly associated with liver cancer patients' prognosis concurrently (Fig. 6a). Then further multivariate Cox regression analysis were performed (Fig. 6b). Finally, five genes including ATIC, BIRC5, BAX, CAPNS1 and FKBP1A were identified as risk genes in OS and to develop prognostic signature. Moreover, the Kaplan–Meier analysis was performed to focus on the prognostic ability of each ARG. The results from the TCGA database indicated that overexpression of ATIC, BIRC5, BAX, CAPNS1 and FKBP1A was closely related to inferior OS of liver cancer patients (Fig. 7a). And similar results were obtained from the ICGC database. However, there was no significant difference in OS with regard to BIRC5 and CAPNS1 expression (Fig. 7b).

Establishment and definition of the prognostic risk model

The risk score formulas for OS-based prognosis were constructed as follows: rick score = (0.5554 × expression value of ATIC) + (-0.3096 × expression value of BAX) + (0.2345 × expression value of BIRC5) + (-0.3780 × expression value of CAPNS1) + (0.5091 × expression value of FKBP1A). Subsequently, the X-tile analysis was performed to determine 1.9 as the optimal cutoff points of risk score in the TCGA set (Fig. 8a-c). Using the cutoff point calculated from the risk score of each patient from the TCGA cohorts, we categorized them into two groups, including a high-risk group and a low-risk group. The risk scores distribution and survival status of patients in TCGA dataset were shown in Fig. 8d. Next, the heat-maps showed the expression profiles of the five risk ARGs (Fig. 8e). We observed that high-risk patients had a higher level of risky genes (ATIC, BIRC5, BAX, CAPNS1 and FKBP1A). The results from ICGC dataset were similar (Fig. 8g).

The correlations between the risk model and clinical parameters in patients with HCC are summarized in Table 1. Furthermore, the results showed that histological grade ($P = 0.029$), pathological T stage ($P < 0.001$) and pathological stage ($P < 0.001$) were closely correlated with the risk score.

Prognostic risk model is an independent predictor of liver cancer

To compare clinical parameters and the independent predictive value of the autophagy-related risk score model, the univariate and multivariate Cox regression models were utilized. In TCGA dataset, the univariate Cox analysis revealed that risk score, tumor stage, T and M stages were correlated with OS of HCC patients (Fig. 9a). And the five-gene risk score remarkably correlated with survival in multivariate Cox regression analysis, whereas other factors were not significant (Fig. 9b). Both univariate and multivariate Cox regression analysis demonstrated that the risk characteristics, tumor gender and stage of patients with liver cancer were markedly correlated with OS in the ICGC dataset (Fig. 9e, f). These results confirmed that the autophagy-related prognostic model could independently predicted liver cancer patient's survival.

The risk score of each patient in the TCGA set was calculated with the five-gene risk score formula. As expected, the risk score classified liver cancer patients into high- and low-risk group based on optimal cutoff point with a significantly different prognosis (Fig. 9c). And the high-risk patients had lower OS than the low-risk patients. The ICGC dataset was treated as an independent external validation and was processed in the same way. The Kaplan–Meier analysis demonstrated that the prognostic ability of the signature once again (Fig. 9g).

With the help of the OS-based ROC curves, the predictive performance of the risk score were assessed. For the risk score of OS in TCGA dataset, the AUC values was 0.746, which was apparently higher than that of age (AUC = 0.524), gender (AUC = 0.504), tumor grade (AUC = 0.501), tumor stage (AUC = 0.678), T stage (AUC = 0.679), M stage (AUC = 0.508), and N stage (AUC = 0.508) (Fig. 9d). Afterwards in the IGCG dataset, the AUC of the signature was also as high as 0.744 (Fig. 9h). These data suggested that the risk score was competitive in the survival prediction of liver cancer patients.

Discussion

HCC is one of the most lethal human cancers. With the development of clinical management of liver cancer, some prognostic factors including tumor volume, grade and stage and the number of lesions are characterized [7, 8]. But, an effective molecular biomarker for HCC prognosis monitoring is still urgently needed. There is an increasingly emerging evidence suggest that autophagy is closely implicated in tumorigenesis and progression [9]. The exploration of mechanism about autophagy opens up a new prospect approaching for liver cancer. In present, high-throughput biological technologies have been widely applied in the early diagnosis of cancer. Therefore, using large-scale databases will help to explore the expression pattern of ARGs and reveal the prognosis of HCC patients.

In the current study, based on the high-throughput expression data from two datasets (TCGC and ICGC), we aimed to screen key ARGs having intimate connection with the prognosis of patients with HCC. Firstly, 22 ARGs were found having differentially expression between liver tumor and normal tissues, including 3 up-regulated and 19 down-regulated genes. The results of GO terms and KEGG pathways analysis showed the major enrichment in tumor biological process and molecular function. It was observed that the KEGG pathways enriched by the differentially expressed ARGs was involved in several types of

cancer. The results suggested that specific autophagy pattern may played a role in occurrence and progression of liver cancer. Then we observed 14 risk ARG related to OS in the TCGA database by dimensionality reduction in univariate survival analysis. And further multivariate survival analysis decided five key prognostic ARGs (ATIC, BAX, BIRC5, CAPNS1, FKBP1A) to construct prognostic risk models, which could provide accurate prognosis for patients with liver malignant tumor. Multivariate Cox regression analysis of prognostic risk model and clinical parameters showed that the five-gene risk score is conducive to independently predict the prognosis of patients with liver cancer. Meanwhile the results of ROC curve analysis suggested that the prognostic risk model could distinguished healthy people from liver cancer patients accurately.

ATIC, a bi-functional protein enzyme, catalyzes the final two steps of the de novo purine biosynthetic pathway. Recent studies have shown that ATIC is expressed at high levels in lung cancer and related to poor patient prognosis [10]. There are few reports on its function in liver cancer. It has reported that up-regulated of ATIC in HCC was correlated with poor survival and it supported propagation of HCC cells by regulating AMPK-mTOR-S6 K1 signature [11].

Bax has been proved to be one of the most widely-characterized participants in autophagy. It is a member of the BCL2 protein family and functions as an apoptotic activator by forming a heterodimer with BCL2. Bax participates in the mitochondria-initiated intrinsic apoptotic signaling and the extrinsic apoptotic pathway that is triggered by transmembrane death receptors [12, 13]. Also, Bax has the effect in the crosstalk between endoplasmic reticulum (ER) signaling pathway and mitochondrial pathways [14]. Considering Bax be important role in apoptosis, it is not unexpected that Bax participates in multiple anticancer drugs that induce apoptosis of cancer cells. SKA3, a component of the spindle and kinetochore-related complexes, influences cell apoptosis by regulation of BAX/Bcl-2 expression in HCC cells [15]. The modulation of MT1G (a low-molecular weight protein with high affinity for zinc ions) on p53 resulted in upregulation of Bax, which leads HCC cells apoptosis [16].

BIRC5 belongs to the inhibitor of apoptosis (IAP) family, which can prevent apoptotic cell death. It has been reported that BIRC5 exerted its influence on HCC cells in promoting proliferation [17]. Recent studies have shown that BIRC5 could be regarded as potential biomarkers for molecular diagnosis as well as therapeutic intervention of HCC and with significant influence on prognosis of HCC patients [18, 19].

CAPNS1, a member of the calpain small subunit family, operate as heterodimers and essential for the calpain activity and function. Several studies have shown that CAPNS1 is associated with biological function to tumorigenesis. Indeed, the expression of CAPNS1 has been detected in various cancers, including hepatocellular carcinoma [20,] ovarian carcinoma [21], colorectal cancer [22], nasopharyngeal carcinoma [23], and other tumors. In vitro experiments found that CAPNS1 enhances the growth and metastasis of HCC by activating FAK-Src signaling pathway and MMP2 [24].

FKBP1A is a cis-trans prolyl isomerase that binds to FK506 and rapamycin, and inhibits calcineurin and the activity of mTOR [25]. FKBP1A was validated to have overexpressed in HCC and predicted the poor

prognosis [26]. However, the specific mechanism of FKBP1A in HCC is still unclear, which deserve to be further investigated.

In summary, there is a close relationship between autophagy and the prognosis of liver cancer patients. In addition, this study suggests that risk ARGs be potential candidates for prognostic biomarkers in HCC with the value to guide making decisions for the choice of clinical treatment. Further researches are needed to provide more specific information about these results. At the same time, based on the discovery of autophagy-related patterns which could impact the prognosis of patients with tumor, our work conducted a risk model to benefit distinguish high-risk liver cancer patients. However, the main limitation of our study is that we used already available data from two public databases, and above results are required to be further investigated in prospective studies.

Abbreviations

HCC, hepatocellular carcinoma; TCGA, The Cancer Genome Atlas; ICGC, International Cancer Genome Consortium; OS, overall survival; ARGs, autophagy-related genes; HADb, Human Autophagy Database; TFs, transcription factors; KEGG, Kyoto Encyclopedia of Genes and Genomes; GO, gene ontology; ROC, receiver operating characteristic; AUC, Area Under Curves.

Declarations

Acknowledgments:

Not applicable.

Authors' contributions:

Conceptualization, W.Y.; software, Z.Z.; validation, Z.S.; resources, Q.Z.; data curation, Z.S.; writing—original draft preparation, W.Y. and Z.S.; writing—review and editing, Q.Z.; supervision, Q.Z.; All authors have read and agreed to the published version of the manuscript.

Funding:

No funding.

Availability of data and materials:

Authors can provide all of datasets analyzed during the study on reasonable request.

Ethics approval and consent to participate:

Not applicable.

Consent for publication:

Not applicable.

Competing interests:

The author reports no conflicts of interest in this work.

Author details:

[1]Department of Surgery, The First Affiliated Hospital, Wenzhou Medical University, Wenzhou, 325015, Zhejiang Province, People's Republic of China.

[2] Key Laboratory of Diagnosis and Treatment of Severe Hepato-Pancreatic Diseases of Zhejiang Province, The First Affiliated Hospital, Wenzhou Medical University, Wenzhou, 325015, Zhejiang Province, People's Republic of China.

*Correspondence:

1.Qiyu Zhang. 2. Bicheng Chen.

E-mail addresses: Qiyuz@126.com(Qiyu Zhang)

References

1. Bray F, Ferlay J, Soerjomataram I, Siegel RL, Torre LA. Jemal A. Global cancer statistics 2018: GLOBOCAN estimates of incidence and mortality worldwide for 36 cancers in 185 countries. Cancer J Clin. 2018;68(6):394–424.
2. Qin JS, Zhang H, Li K, Zhang B. X, Targeting autophagy in chemotherapy-resistant of hepatocellular carcinoma. American journal of cancer research. 2018;8(3):354–65.
3. Xiong H, Ni Z, He J, et al. LncRNA HULC triggers autophagy via stabilizing Sirt1 and attenuates the chemosensitivity of HCC cells. Oncogene. 2017;36(25):3528–40.
4. Jassey CJT, Liu A. CH, et al., Targeting Autophagy Augments BBR-Mediated Cell Death in Human Hepatoma Cells Harboring Hepatitis C Virus RNA. Cells, 2020. 9(4).
5. Liu NW, Liu H. G, et al., Yeast β-D-glucan exerts antitumour activity in liver cancer through impairing autophagy and lysosomal function, promoting reactive oxygen species production and apoptosis. Redox Biol. 2020;32:101495.
6. Niture S, Gyamfi MA, Lin M, et al. TNFAIP8 regulates autophagy, cell steatosis, and promotes hepatocellular carcinoma cell proliferation. Cell death disease. 2020;11(3):178.
7. HM Zakaria
HM Zakaria; Macshut M, Gaballa NK, et al, Total tumor volume as a prognostic value for survival following liver resection in patients with hepatocellular carcinoma. Retrospective cohort study. Annals of medicine and surgery (2012), 2020. 54: p. 47–53.

8. Liu JH, Li FC, Zhou L, Jiang WP, Pan BG. ZY, Nomograms to predict the long-time prognosis in patients with alpha-fetoprotein negative hepatocellular carcinoma following radical resection. Cancer medicine. 2020;9(8):2791–802.
9. Huang F, Wang BR. Wang YG. Role of autophagy in tumorigenesis, metastasis, targeted therapy and drug resistance of hepatocellular carcinoma. World journal of gastroenterology. 2018;24(41):4643–51.
10. Zhu; Wang J, Hu M. D, Development of an autophagy-related gene prognostic signature in lung adenocarcinoma and lung squamous cell carcinoma. PeerJ. 2020;8:e8288.
11. Li M, Jin C, Xu M, Zhou L, Li D. Yin Y, Bifunctional enzyme ATIC promotes propagation of hepatocellular carcinoma by regulating AMPK-mTOR-S6 K1 signaling. Cell communication and signaling: CCS, 2017. 15(1): p. 52.
12. Liu Z, Ding Y, Ye N, Wild C, Chen H. Zhou J. Direct Activation of Bax Protein for Cancer Therapy. Medicinal research reviews. 2016;36(2):313–41.
13. Ramonet MV, Perier D. C, Mitochondrial alterations in Parkinson's disease: new clues. Journal of neurochemistry. 2008;107(2):317–28.
14. Zhou JSu, Xia L, Xu MH, Xiang Y, Sun XY LK, Bcl-2 family proteins are involved in the signal crosstalk between endoplasmic reticulum stress and mitochondrial dysfunction in tumor chemotherapy resistance. BioMed research international, 2014. 2014: p. 234370.
15. Wang YH, Huang Z. S, et al., SKA3 Promotes tumor growth by regulating CDK2/P53 phosphorylation in hepatocellular carcinoma. Cell death disease. 2019;10(12):929.
16. Wang Y, Wang G, Tan X, et al. MT1G serves as a tumor suppressor in hepatocellular carcinoma by interacting with p53. Oncogenesis. 2019;8(12):67.
17. Li LC, Shen C. S, et al., OCT4 increases BIRC5 and CCND1 expression and promotes cancer progression in hepatocellular carcinoma. BMC Cancer. 2013;13:82.
18. Z Wan; Zhang X, Luo Y, Zhao B. Identification of Hepatocellular Carcinoma-Related Potential Genes and Pathways Through Bioinformatic-Based Analyses. Genetic testing molecular biomarkers, 2019. 23(11): 766–77.
19. Wu P, Xiao Y, Guo T, et al. Identifying miRNA-mRNA Pairs and Novel miRNAs from Hepatocelluar Carcinoma miRNomes and TCGA Database. J Cancer. 2019;10(11):2552–9.
20. Chen XBZ, Xu XB. LL, et al., miR-203 inhibits augmented proliferation and metastasis of hepatocellular carcinoma residual in the promoted regenerating liver. Cancer Sci. 2017;108(3):338–46.
21. Yang X, Sun J, Xia D, et al., Capn4 Enhances Osteopontin Expression through Activation of the Wnt/β-Catenin Pathway to Promote Epithelial Ovarian Carcinoma Metastasis. Cellular physiology and biochemistry: international journal of experimental cellular physiology, biochemistry, and pharmacology, 2017. 42(1): p. 185–197.
22. Li J, Xu J, Yan X, Jin K, Li W. Zhang R, Suppression of Capn4 by microRNA-1271 impedes the proliferation and invasion of colorectal cancer cells. Biomedicine & pharmacotherapy = Biomedecine

& pharmacotherapie, 2018. 99: p. 162–168.
23. Chen PZ, Xie X. J, et al., Capn4 is induced by and required for Epstein-Barr virus latent membrane protein 1 promotion of nasopharyngeal carcinoma metastasis through ERK/AP-1 signaling. Cancer Sci. 2020;111(1):72–83.
24. Dai Z, Zhou SL, Zhou ZJ, et al. Capn4 contributes to tumour growth and metastasis of hepatocellular carcinoma by activation of the FAK-Src signalling pathways. J Pathol. 2014;234(3):316–28.
25. Chen H, Zhang W, Sun X, et al. Fkbp1a controls ventricular myocardium trabeculation and compaction by regulating endocardial Notch1 activity. Development. 2013;140(9):1946–57.
26. Lin YL, Zhang J, Dai Y, Li G, Liu A X, LncRNA PCAT6 predicts poor prognosis in hepatocellular carcinoma and promotes proliferation through the regulation of cell cycle arrest and apoptosis. Cell biochemistry and function, 2020.

Table

Due to technical limitations, Table 1 is provided in the Supplementary Files section.

Figures

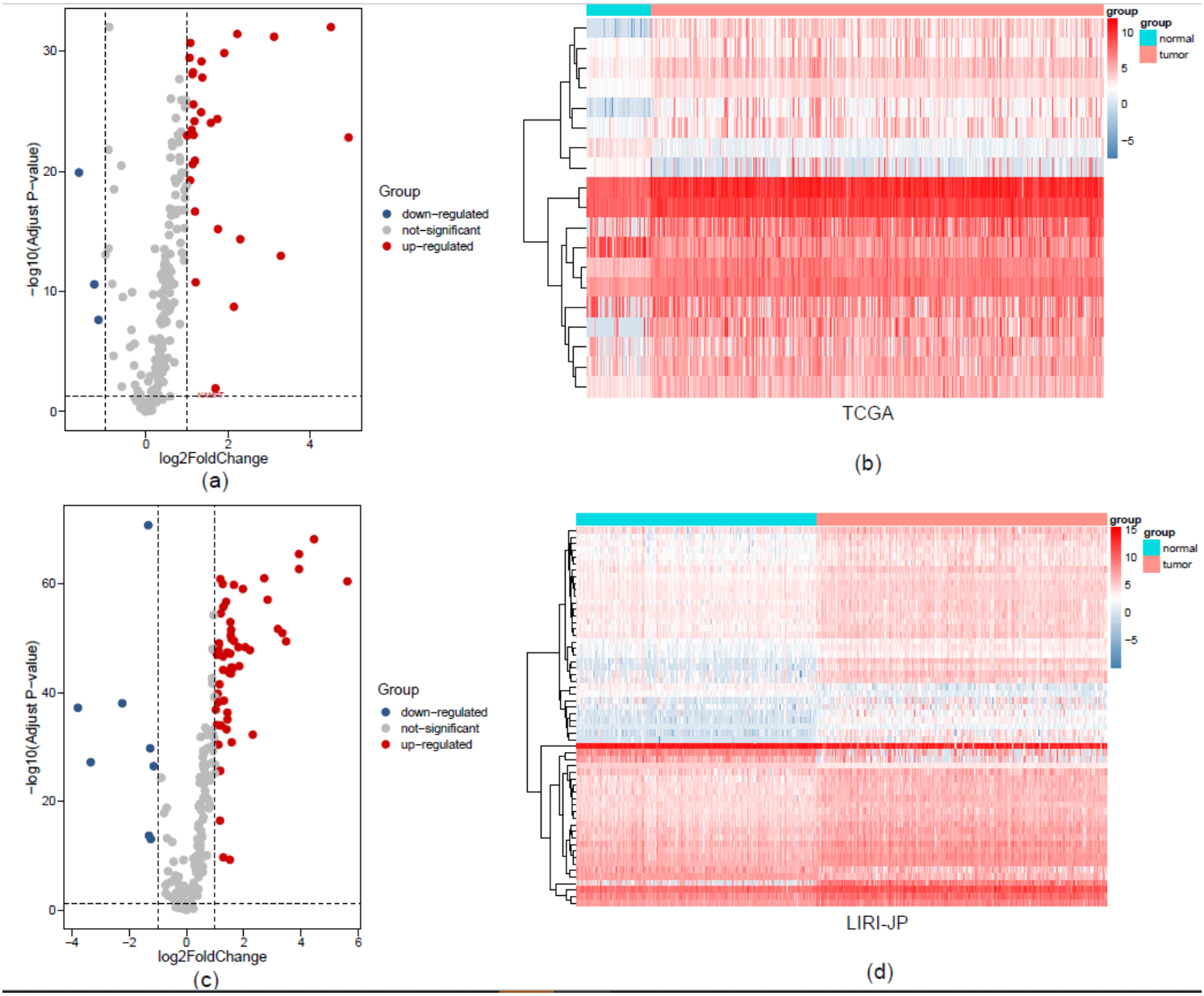

Figure 1

Differential expression of autophagy-related genes (ARGs) between liver cancer and normal liver tissues in two databases. (a) The volcano plot and (b) clustering analysis of differentially expressed ARGs for TCGA data portal. (c) The volcano plot and (d) clustering analysis of differentially expressed ARGs for ICGC data portal. Each point represents a gene. The red dots represent significantly upregulated ARGs and the blue dots represent significantly downregulated ARGs. Each column represents one sample, and each row represents one gene.

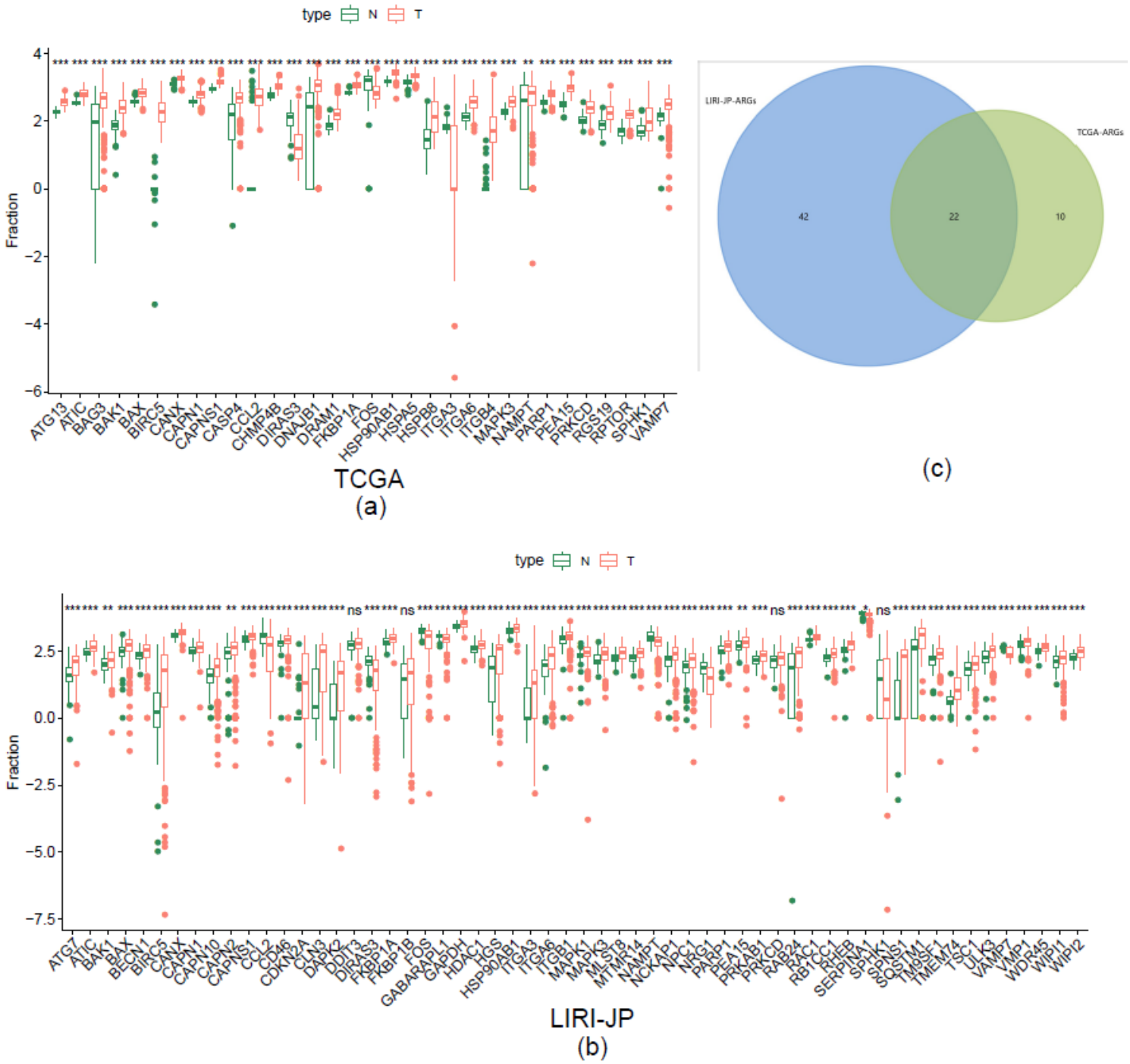

Figure 2

The expression patterns of differentially expressed autophagy-related genes (ARGs) in liver cancer and normal liver tissue in two databases. (a) The expression patterns of TCGA dataset. (b) The expression patterns of ICGC dataset. (c) Venn diagrams of the overlapping differentially expressed ARGs between TCGA and ICGC database, including 3 significantly up-regulated genes and 19 significantly up-regulated genes.

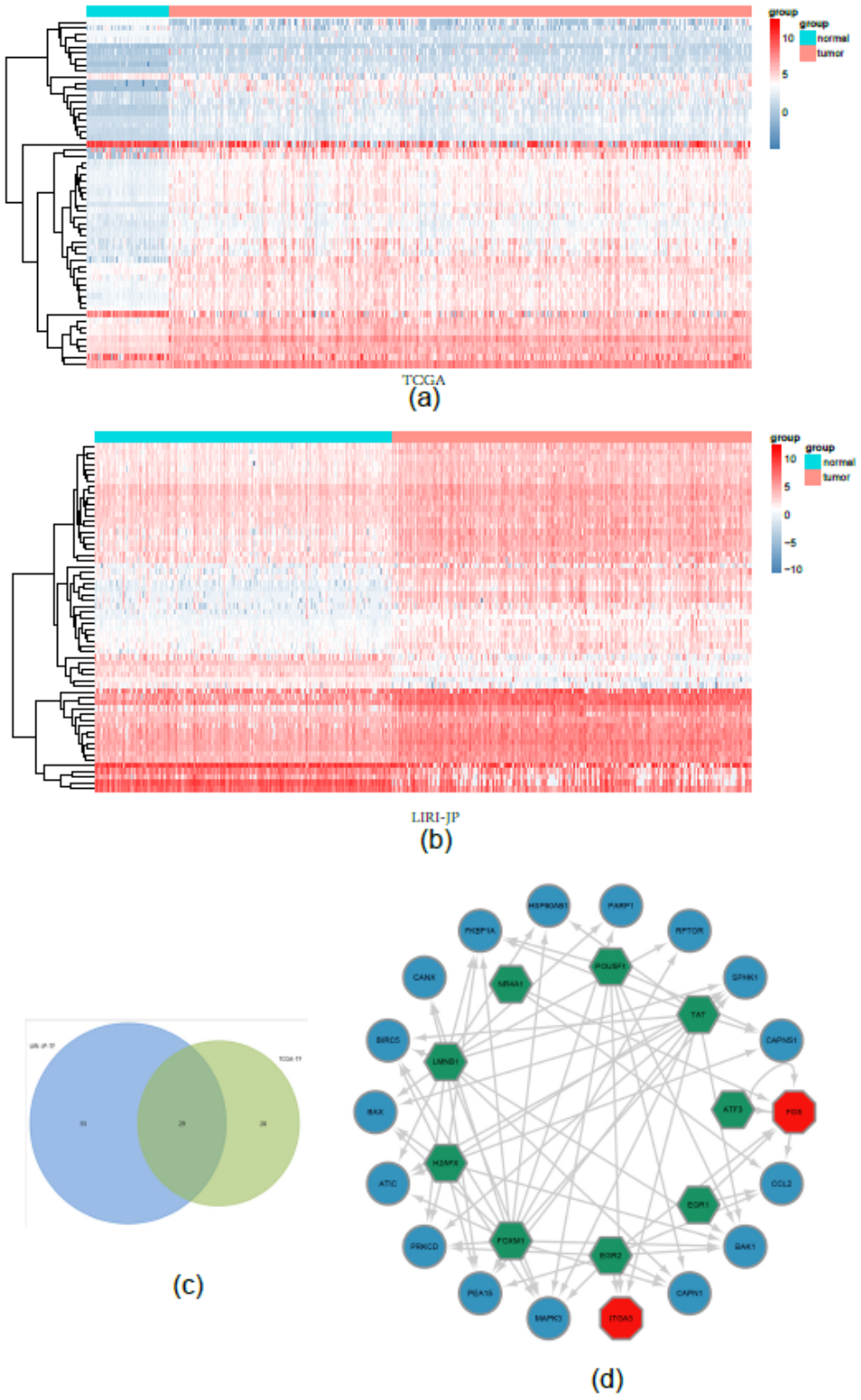

Figure 3

Co-expression network of the differentially expressed transcription factors (TFs) genes and differentially expressed autophagy-related genes (ARGs). (a), (b) The clustering analysis of differentially expressed TFs for TCGA and ICGC data portal respectively. (c) Venn diagrams of the overlapping differentially expressed TFs between TCGA and ICGC dataset. (d) The co-expression network. Green hexagons represent TF genes, blue circles represent low-risk ARGs, and red octagons represent high-risk ARGs.

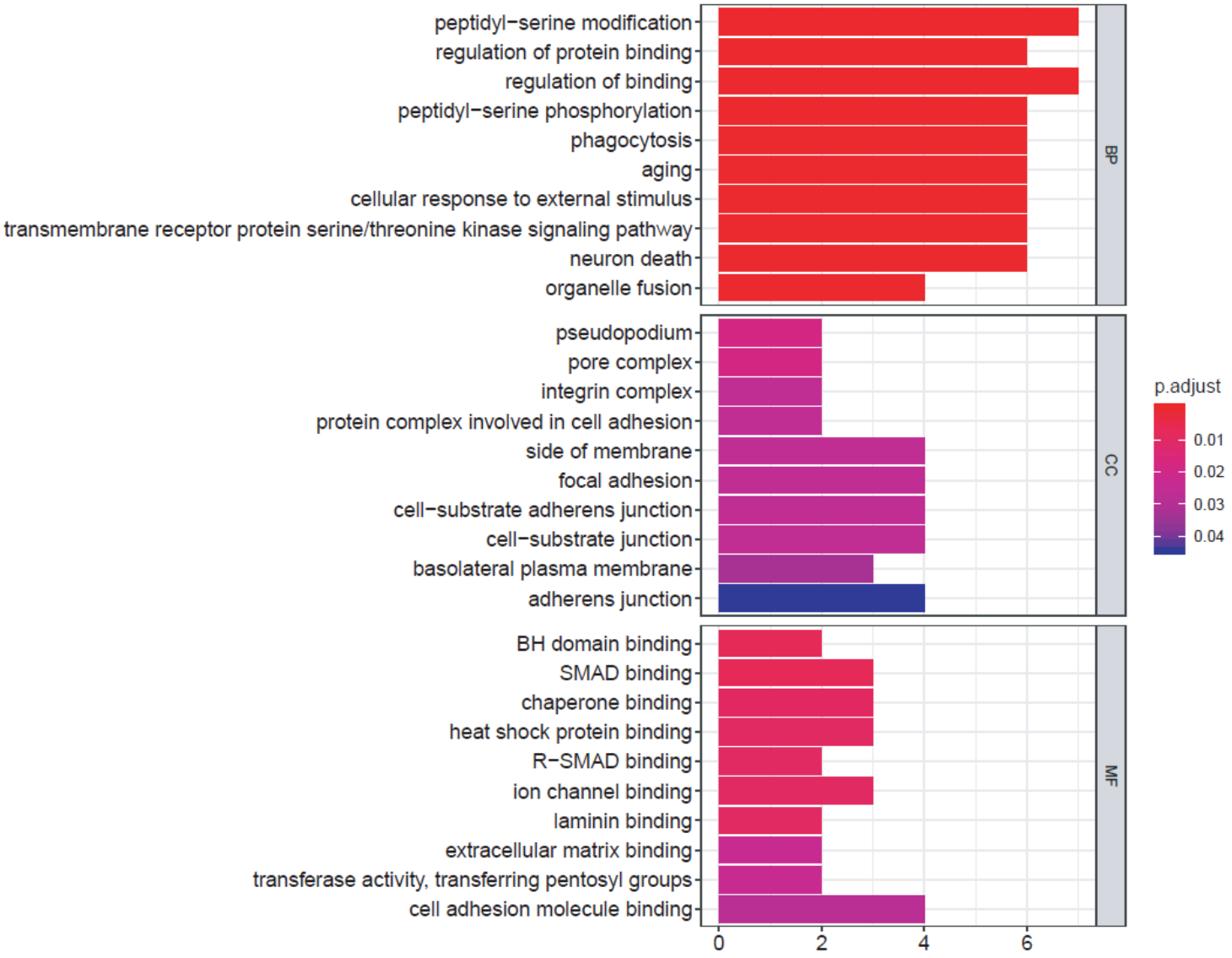

Figure 4

The barplot of enriched gene ontology (GO) terms. BP indicated biological process; CC indicated cellular component; MF indicated molecular function.

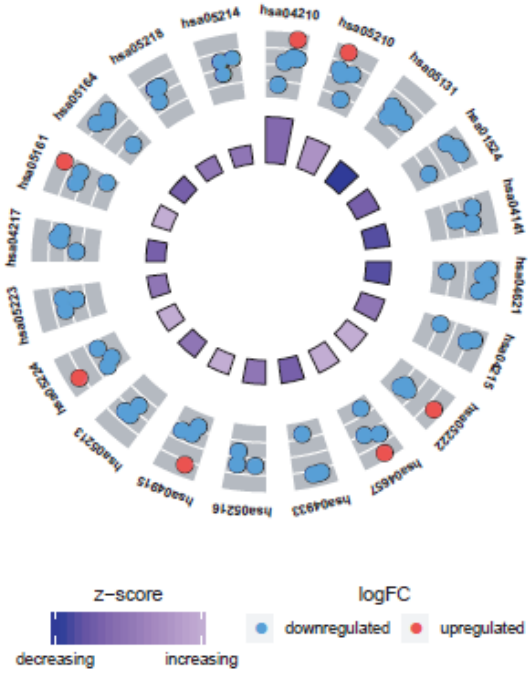

ID	Description
hsa04210	Apoptosis
hsa05210	Colorectal cancer
hsa05131	Shigellosis
hsa01524	Platinum drug resistance
hsa04141	Protein processing in endoplasmic reticulum
hsa04621	NOD−like receptor signaling pathway
hsa04215	Apoptosis − multiple species
hsa05222	Small cell lung cancer
hsa04657	IL−17 signaling pathway
hsa04933	AGE−RAGE signaling pathway in diabetic complicati
hsa05216	Thyroid cancer
hsa04915	Estrogen signaling pathway
hsa05213	Endometrial cancer
hsa05224	Breast cancer
hsa05223	Non−small cell lung cancer
hsa04217	Necroptosis
hsa05161	Hepatitis B
hsa05164	Influenza A
hsa05218	Melanoma
hsa05214	Glioma

(a)

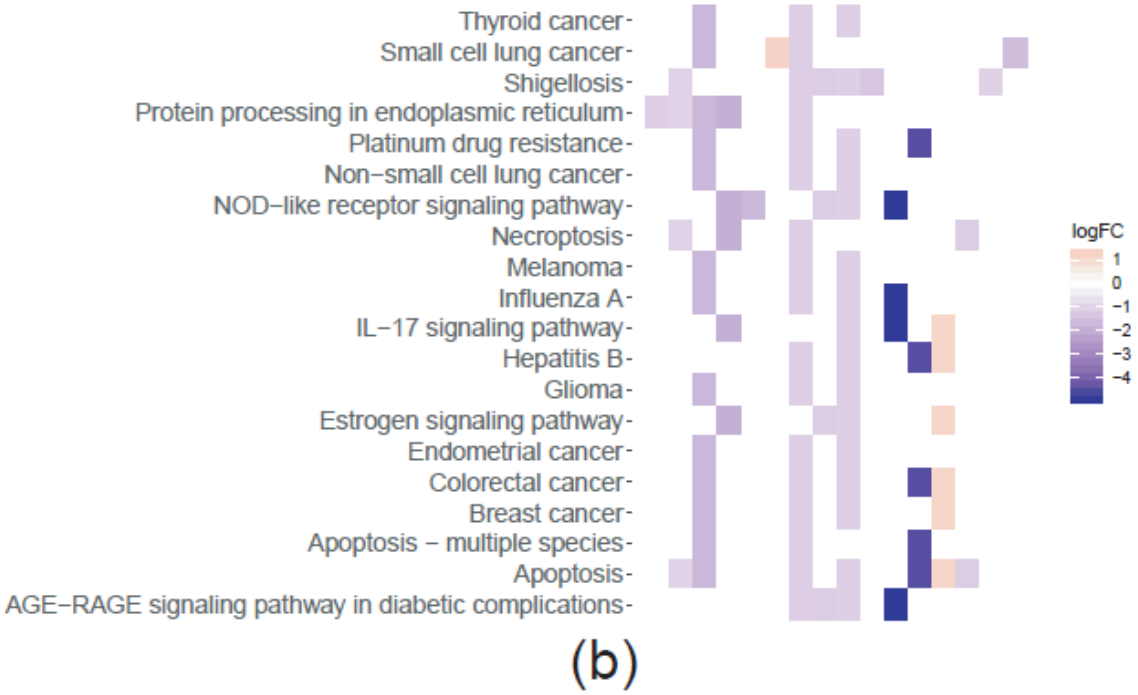

(b)

Figure 5

The Kyoto Encyclopedia of Genes and Genomes (KEGG) pathway-enrichment analysis of differentially expressed autophagy-related genes (ARGs). (a) The circle shows a scatter plot for each term of the logFC of the assigned genes. The red circles represent up-regulation, and the blue ones represent down-regulation. (b) The heat map of the relationship between ARGs and pathways. The color of each block depends upon the values of logFC.

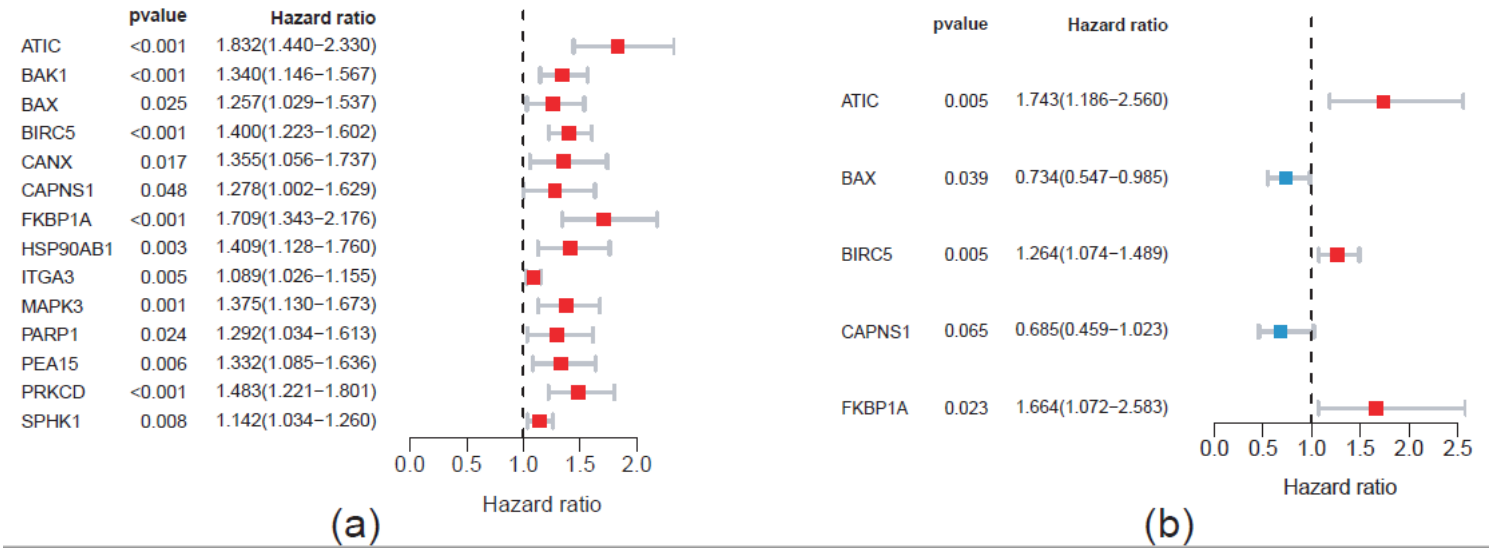

Figure 6

The autophagy-related prognostic genes of liver cancer patients. The (a) univariate and (b) multivariate Cox regression analysis revealed the pool of the prognosis-related genes.

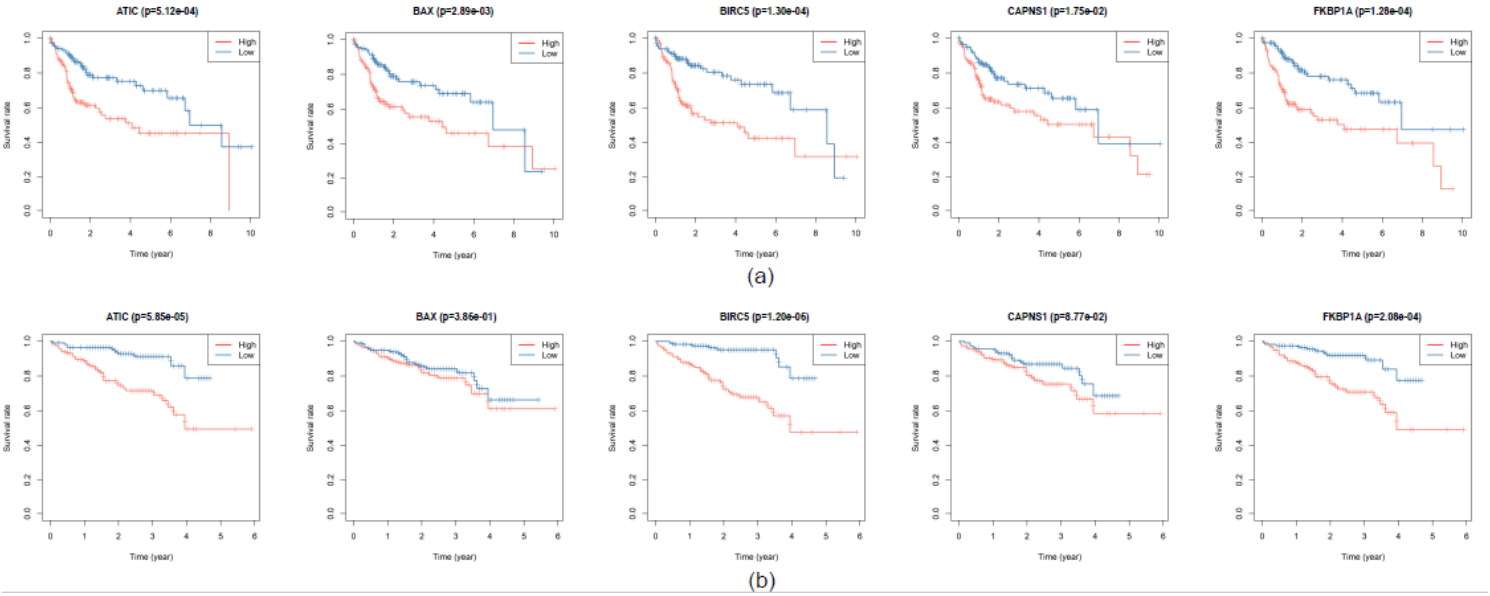

Figure 7

The correlation between screened autophagy-related genes (ARGs) and overall survival (OS) of liver cancer patients. (a) Kaplan-Meier survival curve analysis in TCGA cohort. (b) Kaplan-Meier survival curve analysis in ICGC cohort.

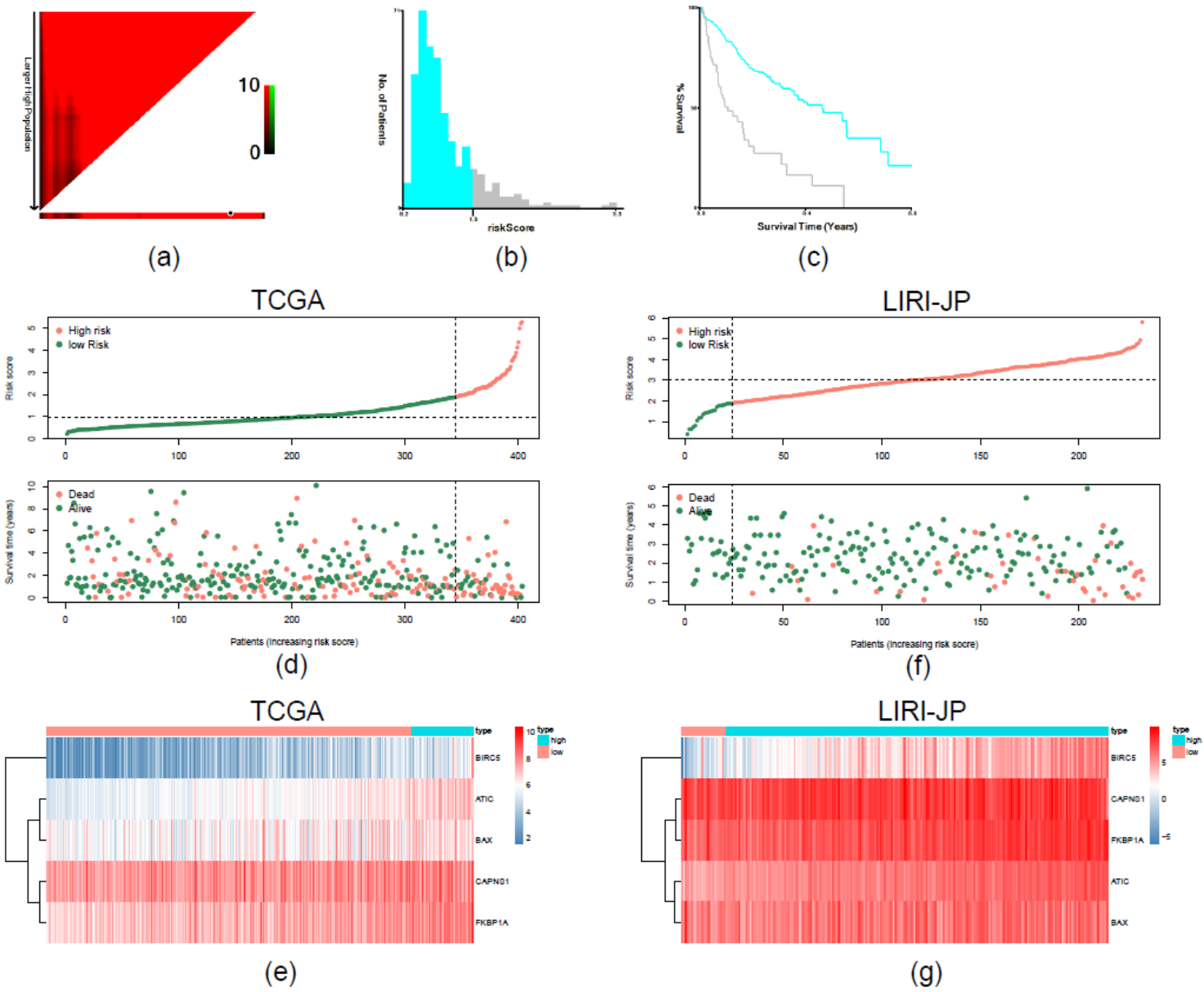

Figure 8

The autophagy-related risk score analysis of HCC patients. X-tile analysis of the prognostic risk score in TCGA training cohort. (a) The X-tile plots of training group. The black circles highlight the optimal cutoff values. (b) Histogram of the entire cohort divided into low-risk score and high-risk score subgroups according to the cutoff value of 1.9. Blue bars represent the low-risk score group, and grey bars represent the high-risk score group. (c) Kaplan-Meier plot of overall survival (OS) in groups stratified using the optimal cut-off value of risk score. Blue curves represent the low-risk score group, and grey curves represent the high-risk score group. (d) The risk score distribution and OS of patients in TCGA database. (e) The heat-map of the five genes expression profiles in TCGA database. (f) The risk score distribution and OS of patients in ICGC database. (g) The heatmap of the five genes expression profiles in ICGC database.

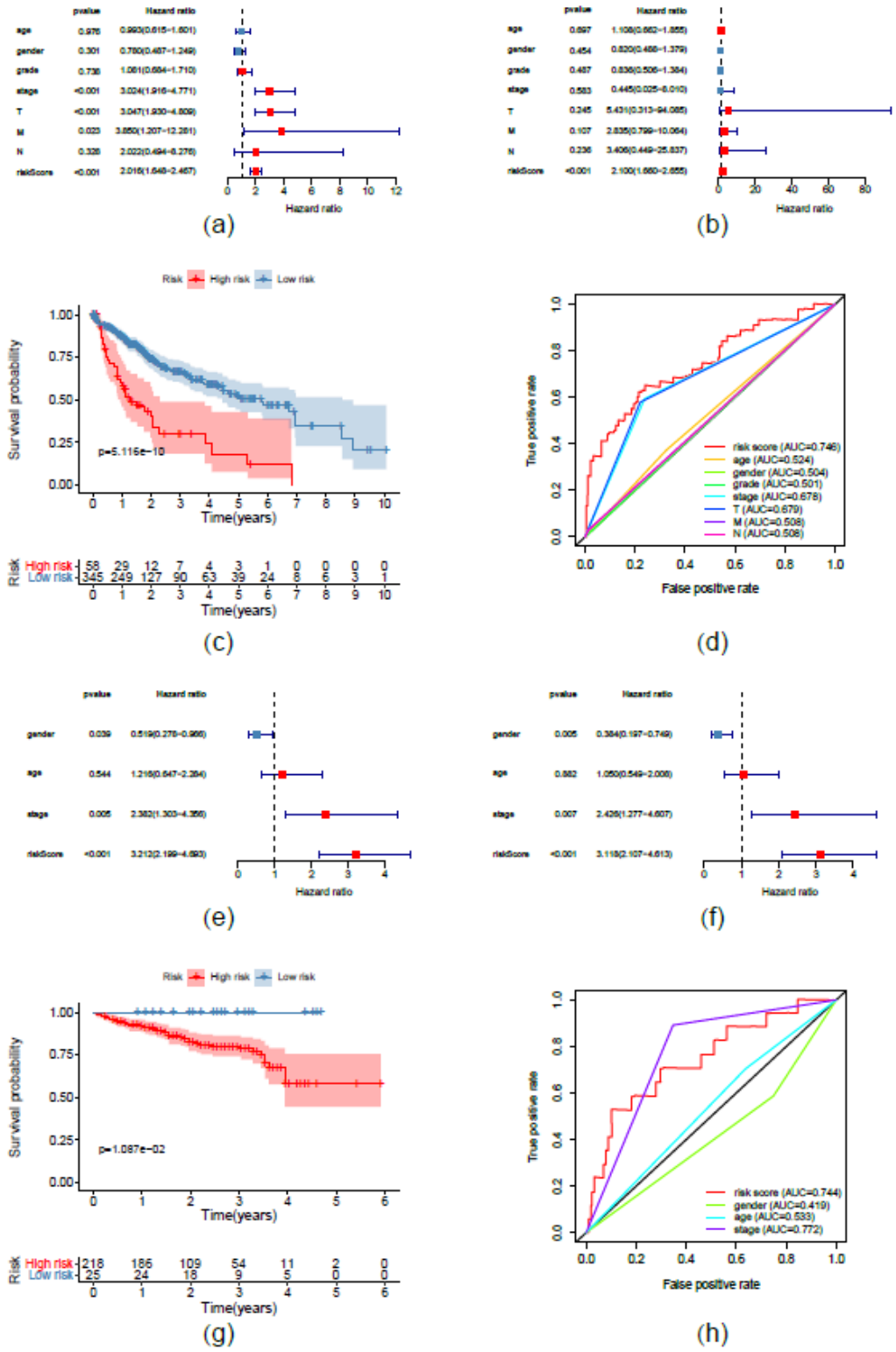

Figure 9

The prognostic value of the five-gene risk score of liver cancer patients. (a, b) The univariate and multivariate Cox regression analyses reveal the independent value of the autophagy-related signature for overall survival (OS) in TCGA database. (c) Kaplan–Meier (K–M) survival curve of OS in the high-risk and low-risk patients based on TCGA database. (d) Time-dependent ROC curve analysis shows AUC value for OS based on TCGA database. (e, f) The univariate and multivariate Cox regression analyses verify the

independent value of the autophagy-related signature for OS in ICGC database. (g) K–M survival curve of OS in the high-risk and low-risk patients based on ICGC database. (h) Time-dependent ROC curve analysis shows AUC value for OS based on the ICGC database.

Supplementary Files

This is a list of supplementary files associated with this preprint. Click to download.

- Table1.pdf